
Article:
Sanver, D, Sadeghpour, A, Rappolt, M orcid.org/0000-0001-9942-3035 et al. (2 more authors) (2020) Structure and Dynamics of Dioleoyl-Phosphatidylcholine Bilayers under the Influence of Quercetin and Rutin. Langmuir. ISSN 0743-7463

https://doi.org/10.1021/acs.langmuir.0c01484

Structure and Dynamics of Dioleoyl-Phosphatidylcholine Bilayers under the Influence of Quercetin and Rutin

Didem Sanver,[1,2] Amin Sadeghpour,[2,3] Michael Rappolt,[2] Florent Di Meo,[4] and Patrick Trouillas[4, 5]

[1]Necmettin Erbakan University, Faculty of Engineering and Architecture, Department of Food Engineering, Konya 42050, Turkey [2]School of Food Science and Nutrition, University of Leeds, Leeds LS2 9JT, UK [3]Biomaterials Science Center, Department of Biomedical Engineering, University of Basel, 4123 Allschwil, Switzerland. [4]INSERM U1248 IPPRITT, Univ. Limoges, 2 rue du Prof. Descottes, 87000 Limoges, France [5]RCPTM, Dpt. Physical Chemistry, Fac. Sciences, Palacký University, Olomouc, Czech Republic

Keywords: Flavonoid, DOPC, biomembrane model, flavonoid-lipid interactions, SAXS, MD simulations.

Abstract: Quercetin and rutin, two widely studied flavonoids with applications foreseen in the sectors of pharmaceutical and cosmetic industries, have been chosen as model compounds, for a detailed structural and dynamical investigation onto their influence on fluid lipid bilayers. Combining global small angle X-ray scattering (SAXS) analysis with molecular dynamics (MD), various changes in the properties of Dioleoyl-Phosphatidylcholine (DOPC) bilayers have been determined. The solubility of quercetin in DOPC membranes is assured up to 12 mol%, whereas rutin, with additional glucose and rhamnose groups, are fully soluble only up to 6 mol%. Both flavonoids induce an increase in membrane undulations and thin the bilayers slightly (< 1 Å) in a concentration dependent manner, wherein quercetin shows a stronger effect. Concomitantly, in the order of 2-4% the adjacent bilayer distance increases with the flavonoid's concentration. Partial molecular areas of quercetin and rutin are determined to be 26 and 51 $Å^2$, respectively. Simulated averaged areas per molecule confirm these estimates. A 60° tilted orientation of quercetin is observed with respect to the bilayer normal, whereas the flavonoid moiety of rutin is oriented more perpendicular (α-angle 30°) to the membrane surface. Both flavonoid moieties are located at a depth of 12 and 16 Å for quercetin and rutin, respectively, while their anionic forms display a location closer to the polar interface. Finally, at both simulated concentrations (1.5 and 12 mol%), DOPC/rutin systems induce a stronger packing of the pure DOPC lipid bilayer, mainly due to stronger attractive electrostatic interactions in the polar lipid head region.

Introduction

There has been a growing interest in the research on natural dietary flavonoids due to their versatile therapeutic potentials in the treatment of several diseases for the past decade. A number of epidemiological and pre-clinical evidence suggest that flavonoids can act as antioxidant, anti-cancer, anti-inflammatory and immune-modulating agents.[1, 2, 3] Aglycone quercetin and its most prominent glycoside form rutin are major flavonoids in the human diet, and they are widely distributed as secondary metabolites in many fruit and vegetables including apples, onions, buckwheat, tea, and wine.[4] Quercetin and rutin have already been marketed as over-the-counter food supplements against allergic inflammation, i.e., allergic rhinitis and asthma, and their curative effects for other diseases are under investigation.[5, 6] Some of these plant-derived natural products are expected to at least partially eliminate side-effects of synthetic drugs while promoting health benefits.

However, relevant pharmacological properties of flavonoids are still matter of ongoing studies and debate, as just recently examined in a systematic review.[7] Questions regarding flavonoid's low absorption and bioavailability, metabolism and the safety of dosage remain big challenges to tackle. For example, most flavonoids are not very soluble neither in water nor in oil, which partly explains their low bioavailability. Recent attempts have focused on improving this bioavailability for flavonoids by encapsulating them into lipid-based formulations to harness their therapeutic potentials. One of the promising delivery systems for encapsulation of flavonoids are liposomes.[8] These nanoscale structures are spontaneously formed as vesicles upon dispersion of phospholipids in water, in which an aqueous volume is entrapped within this lipid self-assembly. These vesicles have been reported to be effective delivery systems for a variety of bioactive molecules from drugs to low-soluble nutrients and allergens.[9, 10] Manufacturing vesicle delivery

systems should ideally offer (i) enhanced biocompatibility, (ii) optimized compound load, and (iii) reduced toxicity at target sites. Moreover, molecules with different physicochemical properties, such as hydrophilicity, hydrophobicity, and amphiphilicity, can all be encapsulated into liposomal formulations, possibly locating at different compartments, namely in the inner aqueous compartment, in between the lipid chains of the membrane, or at the inner lipid-aqueous interface. Liposomes in the form of vesicles can also be designed to mimic biomembranes,[11] which may facilitate their delivery action at the biological target.

Biomimetic membranes, whose composition and morphology can be perfectly tailored, provide highly versatile models to study the interactions between flavonoids and the lipid membranes of liposomes. Considering their easy formulation at reduced costs compared to working with living cells, such artificial membranes can serve new pharmaceutical developments, allowing to study the effects of incorporated bio-molecules in a lipidic environment. For example, when flavonoids partition in biomembranes, they may change their physical properties such as fluidity/rigidity and thickness. Understanding the way flavonoids change these parameters is of significant importance as this may be (in)directly linked to therapeutic potentials, as seen by the observed impact of some flavonoids on fluidity.[12] Another example of a key biological action of flavonoids directly attributed to their impact on biomembranes is their capacity to influence the lifetime of model ion channels, such as gramicidin A.[13, 14]

In our previous work, we provided (i) a summative view about the current knowledge available on flavonoid interactions with planar membranes, established (ii) a structure-activity relationship between flavonoids and monolayer model systems through supported monolayers on Pt/Hg electrode, and observed (iii) the film stability through free-standing monolayers at an air-water interface. [10] In a complementary approach, this paper will report on the quantitative analysis of

the interactions between two prototypical flavonoids, quercetin and rutin (Figure 1) and multilamellar vesicles (MLVs) of Dioleoyl-Phosphatidylcholine (DOPC), using Small-Angle X-ray Scattering (SAXS). The aim of this study is to access detailed information on (i) bilayer structural changes such as membrane thickness, water layer thickness (the distance between adjacent bilayers), and (ii) mechanical properties concerning bilayer fluidity and undulations in the presence of quercetin and rutin. To get a better insight into the localization and orientation of flavonoids within the DOPC bilayer, molecular dynamic (MD) simulations were carried out, which also provided information about membrane alteration in the presence of both quercetin and rutin in their charged and neutral forms.

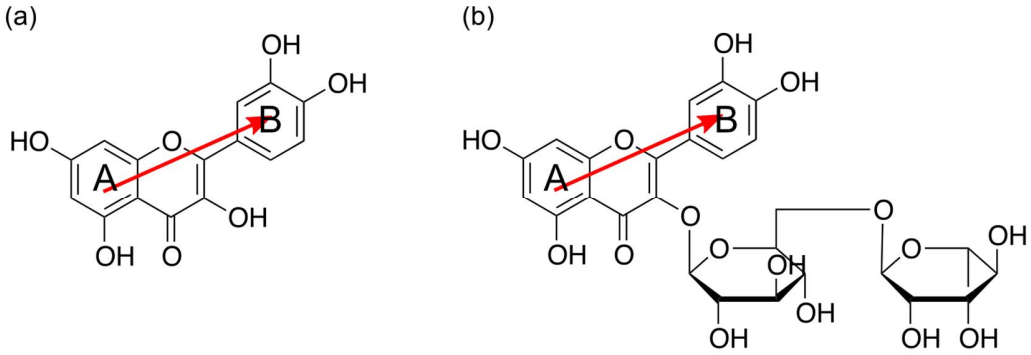

Figure 1. Two-dimensional view of the chemical structure of quercetin (a) and rutin (b). Note, red arrows between two phenyl rings (A and B) of flavonoid skeleton define vectors used to calculate molecular orientation with respect to the z-axis, perpendicular to membrane surface (rf. to MD simulations).

Materials and Methods

Sample Preparation for the X-ray Experiments

1,2-dioleoyl-*sn*-glycero-3-phosphocholine (DOPC) with the purity of > 99% was purchased from Avanti Polar Lipids (USA). Quercetin dihydrate and rutin trihydrate (quercetin-3-β-D-rutinoside) were supplied by Sigma-Aldrich (Germany). Phosphate buffered saline (PBS) powder was obtained from Sigma-Aldrich and used to prepare the pH 7.4 buffer solution using deionised water (Millipore Inc., Ω = 18.2 MΩ.cm) to achieve 0.01 M PO_4^{3-}, 0.138 M NaCl and 0.0027 M KCl. Ethanol (absolute, AR, Merck) was used as received without further purification. For the X-ray experiments, MLVs were prepared according to standard protocols.[15] Briefly, a DOPC stock solution was made by dissolving 10 wt. % of lipid in ethanol. The quercetin- and rutin-containing stock solutions were also prepared by dissolution in ethanol and then each mixed with the DOPC solution resulting in a range of concentration 0-24 mol%. Each mixture was vortexed for 2 minutes and the solvent was evaporated in a vacuum oven for 24 h at 30 °C at 0.01 mbar to secure that all traces of EtOH were removed. After obtaining dry thin films at the bottom of the sample tube, appropriate amounts of diluted buffer solution (90 µL) with 0.1 mM ionic strength and a pH 7.1 (PBS buffer diluted 100x to prevent osmotically induced inhomogeneity of MLV bilayer stacking) was added into the sample tube to fully hydrate the films and were continuously vortexed for half an hour to fully hydrate the film and form MLVs.

X-ray scattering experiments

The SAXSpace instrument (Anton Paar, Graz, Austria) is equipped with a sealed-tube Cu anode X-ray generator. It was operated at 40 kV and 50 mA and chilled by a closed water circuit. The line-focus camera (Anton Paar, Graz, Austria) uses Cu-Kα radiation with a wavelength λ =

0.154 nm. For current experiments, the minimum accessible scattering vector value, q_{min}, was 0.05 nm^{-1} ($q = 4\pi/\lambda \sin(\theta)$, where 2θ is the scattering angle). Silver behenate with a known lamellar spacing of 5.84 nm was used to calibrate the scattering vector modulus q.[16] In order to identify the precise position of the primary beam and the transmission correction of the scattering profiles, a semi-transparent beam stop was used.

Reusable vacuum-tight quartz capillary (Anton Paar, Graz, Austria) with an outer diameter of 1 mm was used to study fluid samples. The temperature was controlled by a remote-controlled sample stage (TCStage 150, Anton Paar, Graz, Austria) with a precision of 0.1 °C. The SAXSpace is equipped with a Mythen micro-strip X-ray detector (Dectris Ltd, Baden, Switzerland). Three separate recordings each with an exposure time of 600 sec were averaged to obtain the final scattering profile.

Background corrected SAXS patterns were analysed by the application of the modified Caillé theory and the evolutionary technique of Particle Swarm Optimization (PSO) has been applied for the global fitting analysis,[17, 18] in order to avoid false local minima fitting solutions. PSO is a modern optimization technique which is inspired by the social behaviour of flocks of birds and its algorithm bases on a population of candidate solutions, called particles, 'flying' through the problem space.[19] In our case, each particle is defined as a multi-dimensional vector with each index representing an input parameter of the fitting routine according to the modified Caillé theory. In addition, we used a batch-fitting approach in which all the experimental patterns obtained during a temperature scan were fitted together Physically meaningful constraints were applied in the batch fitting, leading to a more precise estimation of the fitting parameters. This included constraints on the fluctuation parameter to increase and the bilayer thickness to reduce by increasing the temperature. The technique and underlying premises have been described

previously in detail.[20, 21] (for a review see reference[22] and refer for further details to the X-ray Scattering Optimization Methods in the Supporting Information). The bilayer model used and its applications have been presented in.[23] Briefly, from the fits to the scattered intensities $I = S(q)|F(q)|^2/q^2$ ($S(q)$: structure factor; $F(q)$: form factor), we directly obtained the lamellar repeat distance d and the headgroup-to-headgroup thickness, d_{HH}. Note that steric bilayer thicknesses are not explicitly discussed in this work, but can easily be obtained by e.g. applying the equation $d_B = d_{HH} + 4\sigma_H$,[21] in which σ_H is the Gaussian peak width applied to the model electron density profile of the headgroup region. The fluctuation or Caillé parameter,[24, 25]

$$\eta = \frac{\pi k_B T}{2d^2 \sqrt{(K_C B)}} \quad (1)$$

was directly obtained from the fits and depends on the membrane bending rigidity, K_C, and the compression bulk modulus, B[26] (k_B denotes the Boltzmann constant, T the temperature and d the lattice spacing). Note that mean fluctuations of the membrane position are proportional to $\sqrt{\eta} \cdot d/\pi$.[27]

The lateral area per molecule calculations for fully hydrated MLVs has been outlined by Hodzic *et al.* [28] As a first step, the molecular volume for each flavonoid was estimated from

$$V_{flav} = \frac{M_w \left(\frac{g}{mol}\right)}{\rho\left(\frac{g}{cm^3}\right) 0.6022} \left(Å^3\right), \quad (2)$$

where Mw is the molecular weight and ρ is the density of flavonoid of interest in the solid state. The calculated molecular volumes for quercetin and rutin are given in Table 1.

Table 1. M_w (g/mol), ρ (g/cm^3), and calculated V_{flav} (Å^3) of quercetin and rutin.

	Quercetin	**Rutin**
$\boldsymbol{M_w}$ **(g/mol)**	302.2	664.6
$\boldsymbol{\rho}$ **(g/cm^3)**	1.80[29]	1.82
$\boldsymbol{V_{flav}}$ **(Å^3)**	279	606

The lateral area per molecule, i.e., including lipids and flavonoids, was determined from

$$A(x) = \frac{2 \cdot V(x)}{d_{Luzzati}(x)} \approx \frac{2 \cdot V(x)}{d_{HH}(x)}, \quad (3)$$

where x is the inserted molecule concentration of flavonoids, V is the effective molecular volume (see below Eq. 4) and $d_{Luzzati}$ is the membrane thickness that is defined by the Gibbs dividing surface [30]. Note that for pure PC bilayers in the fluid phase, $d_{Luzzati}$ has nearly the same value as d_{HH} [31]. The influence of insertion of the flavonoids into the bilayers onto the Gibbs dividing surface was not considered. In the case of linear dependence of $A(x)$ one can extract estimates for the partial molecular areas A_{PC} and A_{flav} by the relation.[32]

$$A(x) = x\, A_{flav} + (1 - x) \cdot A_{PC} \quad (4)$$

The effective volumes of DOPC/Flavonoid bilayer systems were estimated using:

$$V(x) = x\, V_{flav} + (1 - x) \cdot V_{PC} \quad (5)$$

Nagle *et al*. published the absolute specific volume of fully hydrated DOPC MLVs; V_{DOPC} = 1303.0 Å^3 at 30 °C.[33] Afterwards, Pan *et al*. reported the temperature dependence of V_{DOPC}.[34] From these literature values, we interpolated V_{DOPC} at 25 °C to be 1298 Å^3. Results of the effective volumes are summarized in **Table 2**.

Table 2. Concentration-dependent effective volume estimates for flavonoids incorporated into DOPC MLVs at 25 °C.

Concentration (mol%)	$V_{eff\_DOPC/Quercetin}$ (Å^3)	$V_{eff\_DOPC/Rutin}$ (Å^3)
0	1298	1298
2	1278	1284
6	1237	1256
12	1176	-

MD Simulations

Force Field Parameters. The Amber force field (FF) Lipid14[35] was used to describe DOPC lipid molecules. The lipid bilayers were solvated by TIP3P[36] water model. FF parameters of the quercetin moiety were derived from GAFF[37] using the antechamber package.[38] Atomic charges were derived from RESP (restrained fit of electrostatic potential) based on calculations achieved within the density functional theory (DFT) formalism with the (*IEFPCM*)-B3LYP/cc-pVDZ method, using diethylether as an implicit solvent.[39] The DFT calculations and the atomic charge fitting were performed with the Gaussian09.RevA[40] and RESP-v.III softwares,[41] respectively. GLYCAM06j-1[42] FF parameters were used to describe the sugar moiety of rutin (i.e., β-D-glucose and α-L-rhamnose). For available Forcefield parameters, please refer to Table S6 in the Supplementary Information.

System builder. A pure DOPC bilayer model made of 128 lipids was created using the membrane lipid builder from the CHARMM-GUI server.[43] The membrane model was solvated with 50 water molecules per one lipid. Na^+ and Cl^- ions were added to match with experimental conditions (i.e., [NaCl] = 0.154 M). MD simulations were carried out using the CPU-PMEMD code available in Amber16.[44, 45] Particle-Mesh-Ewald MD simulations were run first on the pure DOPC lipid bilayer, which was carefully prepared as follows: minimisation of water molecules prior to entire system minimisation; slow thermalisation of water molecules up to 100 K in the

(*N,V,T*) ensemble for 200 ps; thermalisation of the whole system up to the final temperature (298.15 K) of the entire system was achieved for 500 ps in the (*N,P,T*) ensemble with a joint pressure Berendsen weak coupling (pressure relaxation time set up at 2 ps). Then, the DOPC lipid bilayer was equilibrated for 230 ns in the (*N,P,T*) ensemble. This membrane model was then used to build the systems including both quercetin and rutin at two different concentrations, 1.5 and 12 mol%, corresponding to 2:128 and 15:128 polyphenol:lipid ratio, respectively.

For the 1.5 mol% polyphenol-containing systems, both the neutral and the 7-OH depronotated polyphenol were considered; these solutes were initially located in bulk water in each side of the lipid bilayer model. Because the pK_a values of the flavonoids are lower than most physiological pH values and the pH of the solutions used here experimentally, the two charge states were modelled to assess the role of pH on polyphenol partitioning. The 12 mol% polyphenol-containing systems were made from equilibrated DOPC lipid bilayer in which two regular 6 point grids were defined at the mid-position of layer thickness. At each point of the grid, lipid molecules were removed according to solute size to prevent unnatural steric clashes but keeping the exactly same number of lipid molecule in each leaflet. The neutral forms of quercetin and rutin were then added at each point of the grid, i.e., 6 and 6 located in the lower and upper leaflet, respectively. Depending on the different solute sizes, the final systems of 12 mol% quercetin- and rutin-DOPC were made as follows: (12:116) and (12:104) polyphenol: DOPC molecule ratio, respectively. Production MD simulations in the (*N,P,T*) ensemble were performed for 500 ns for each system. Analyses were carried out over the last 200 ns.

Results and Discussion

Structural Changes of the Bilayer upon Lipid-Flavonoid Interaction

SAXS experiments were performed to characterize the membrane structure of both pure and flavonoid-loaded (fully hydrated) DOPC MLVs. In Figure 2, background subtracted SAXS data and corresponding fitted curves are shown for the two systems recorded at room temperature (25 °C). All scattering patterns were globally fitted to extract structural and mechanical features of the membranes. While not shown in Figure 2, this analysis was also carried out temperature dependent as reported in Figures 3 and 4. Structural behaviour of DOPC MLVs compares well with the literature findings on similar bilayer systems over a range of temperature from T = 15 °C to 45 °C. [34] Augmenting the temperature creates an increase in the water layer thickness and membrane undulations of DOPC bilayer (both by about 5%), as well as a decrease in the membrane thickness (by 1.5 %). The reduction in the bilayer thickness of DOPC membranes follow a linear behaviour, which leads to obtaining the thermal expansion coefficient of -5.5×10^{-4} K^{-1}. Similar membrane behaviour, e.g., increased fluctuations at higher temperatures has also been reported for other fully hydrated vesicles comprising 1,2-dimyristoyl-sn-glycero-3-phospho-choline (DMPC),[46] and 1-palmitoyl-2-oleoyl-sn-glycero-3-phosphocholine (POPC). [47, 48 49] The increase in bilayer fluctuations is mainly governed by a progressive decrease of the bilayer bending rigidity modulus, K_C.[34, 48]

Quercetin was incorporated into DOPC MLVs over a range of concentration from 1 mol% up to 24 mol%. As shown in Figure 2A, typical scattering patterns of SAXS for DOPC MLVs were well-maintained in the presence of quercetin up to 12 mol%, and in the presence of rutin up to 6 mol% (Figure 2B), indicating a perfect incorporation of these flavonoids within vesicles. As seen in Figure 2, an additional scattering contribution with an upturn at low q values was observed at

higher quercetin content (at 24 mol%) and rutin (at 12 and 24 mol%). Such additional diffuse scattering contribution most probably accounts for an exceeded solubility of quercetin and rutin, since insolubilized flavonoid crystals are expected to scatter at low q (q_{min} = 0.05 nm^{-1} in our set-up), referring to crystallite sizes greater than 0.1 µm (Figure S1 in the Supporting Information). In order to prevent any misinterpretations that might arise from coexisting flavonoid crystallites, the structural analysis of quercetin and rutin by SAXS are restricted to 12 mol% and 6 mol% concentrations, respectively.

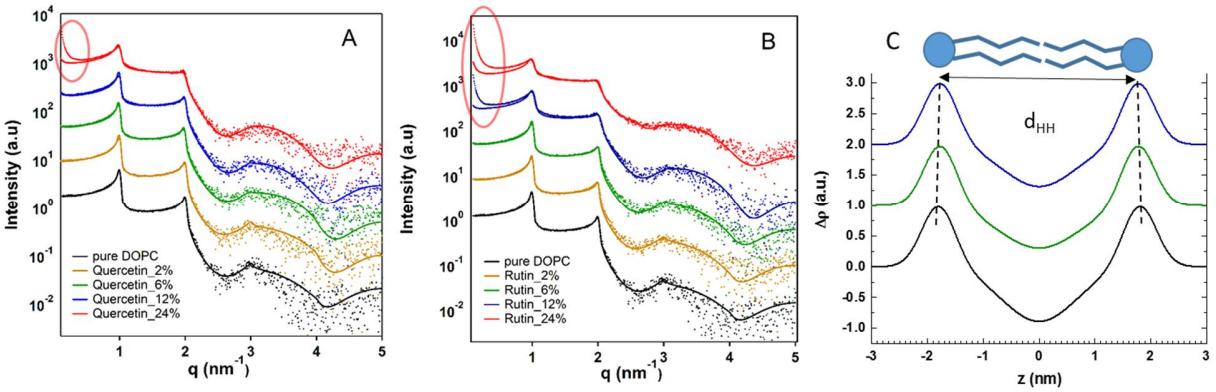

Figure 2. Background subtracted SAXS data, and corresponding fitted curves (solid lines) recorded at 25 °C in PBS (pH 7.0). A.) Pure DOPC MLVs (black) and quercetin-loaded MLVs. B.) Pure DOPC MLVs (black) and rutin-loaded MLVs. Note, red circled regions display diffuse scattering arising from coexisting crystallites (see Figure S1 in the Supporting Information). C.) Three electron density profiles are displayed. From bottom to top DOPC (black), DOPC with 6 mol% rutin (green) and DOPC with 12 mol% quercetin (blue), all recorded at 25 °C. Note, subsequent EDPs are shifted for clarity by 1 and 2 units, respectively. Further, the maximum electron density of the head group is normalised to unity.

The effect of quercetin on the structural parameters, extracted from the global analysis fits (see Figure 2C for electron density profiles of DOPC MLVs with and without quercetin), intensified as a function of increased concentration and temperature as shown in Figure 3. Despite slight influence of quercetin on lattice spacing, d, (less than 1% variation), a visible membrane thinning effect (smaller dHH) is demonstrated in a concentration and temperature dependent manner

(Figure 2C and Figure 3B). This decrease in dHH is accompanied by an increase in the water layer thickness, dW (Figure 3C), and a concomitant increase also in the membrane fluctuation parameter, η (Figure 3D), as also observed for other MLV systems [50,51].

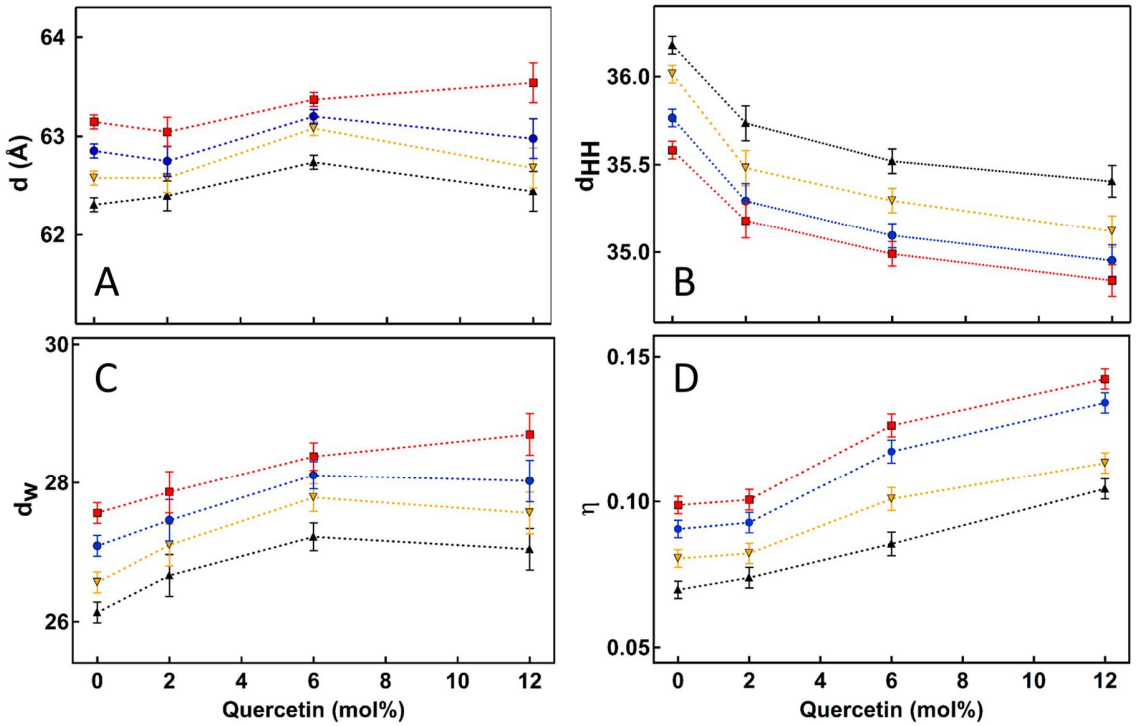

Figure 3. Membrane parameters, d, d_{HH}, d_W and η (A-D) as a function of temperature and quercetin concentration. Black, yellow, blue and red lines are temperature lines at 15, 25, 37 and 45 °C, respectively.

Structural parameters of DOPC MLVs in the absence and presence of rutin (up to 6 mol%) are displayed in **Figure 4**. The influence of rutin on the structural parameters of DOPC MLVs was not as strong as for quercetin. Even at the concentration of 6 mol%, the impact of rutin is relatively weak, which changes the bilayer thickness over the entire range of the flavonoid's concentration only a few tenth of an Å (**Figure 4B**). Alike pure DOPC membranes, the temperature response of the membranes with incorporated flavonoids demonstrate a linear reduction in membrane thickness as a function of increasing temperature. Yet, the induced

changes seem to be less responsive, i.e. the linear expansion coefficient decrease to 5.0×10^{-4} and 4.7×10^{-4} K^{-1} for membranes containing 6 mol% quercetin and rutin, respectively (for further details see Table S2 in the Supporting Information).

Existing studies with model membranes using different characterization methods and MD simulations also suggest that the insertion of a flavonoid into a lipid bilayer can result in changes of membrane thickness.[52, 53, 54] For example, a MD simulation study reported quercetin-triggered deformations on the surface of a DOPC membrane, which resulted in the creation of small cavities embedding water molecules and quercetin molecules, resulting in a local decrease in the membrane thickness.[52]

Green tea catechin derivatives have also been reported to create a membrane thinning effect.[55, 56] Sun and co-workers for example, measured the bilayer thickness of vesicles made from three different lipids (namely DOPC, POPC and egg PC) in the presence of epigallocatechin gallate (EGCG), using X-ray diffraction. Membrane thickness alterations were measured via X-ray diffraction as a function of EGCG/lipid ratio, and EGCG was found to thin the membrane for each model system studied. Similarly, the same group reported a decrease in bilayer thickness upon incorporation of curcumin into DOPC bilayers.[14]

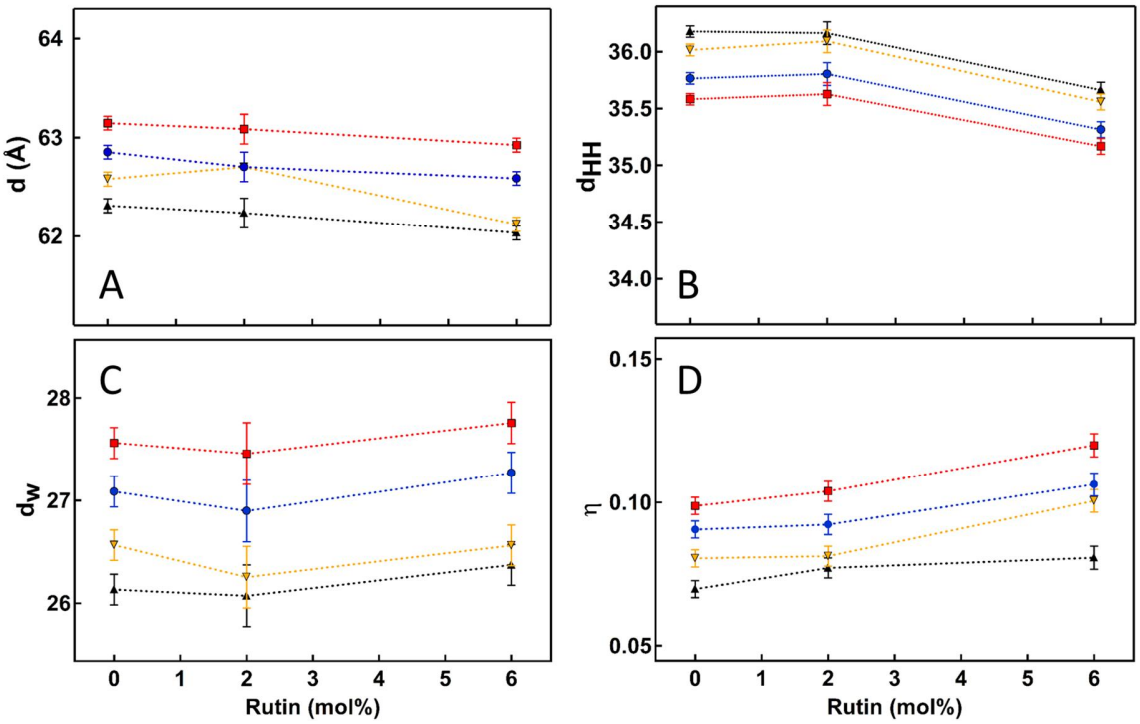

Figure 4. Membrane parameters, d, d_{HH}, d_W and η (A-D) as a function of temperature and rutin concentration. Black, yellow, blue and red lines are temperature lines at 15, 25, 37 and 45 °C, respectively.

An interesting side-topic concerns the influence of bilayer thickness alterations being associated with ion channel activity.[13, 14, 57, 58] The two isoflavonoids, daidzein and genistein, were seen to increase the lifetimes of the gramicidin A (gA) ion channel.[13] One proposed mechanism bases on the ability of flavonoids to reduce the bending modulus, K_C, of the model membranes. This results in a softer and more easily deformable bilayers, which in turn reduces the energy to overcome the hydrophobic mismatch between an ion channel and the surrounding lipid bilayer. Following this view, quercetin and rutin are expected to behave similarly, since both flavonoids were seen to induce bilayer thickness and fluidity changes (cp. **Figure 3** and **4**) and since we observe a monotonous increase in bilayer undulations as a function of flavonoid concentration, which are dependent on K_C (cp. **Eq. 1** and **Figures 3D** and **4D**). The other

mentioned mechanism explains an increase in ion channel lifetimes with the isoflavonoid's ability to thin the bilayer membranes. Thin membrane regions could increase the attractive interactions between gA dimers and isoflavonoids, and as a result of enhance ion-channel stability, its lifetime is expected to increase as well.[13] Noteworthy, also curcumin has been reported to increase the single-channel lifetime of gA in DOPC bilayers without altering the single-channel conductance.[59] Another study further showed a concentration-dependent nonlinear membrane thinning along with a reduced elasticity moduli of the bilayers, when curcumin gets added.[14]

The ability of flavonoids to modify membrane fluidity is also particularly important, since alterations in membrane fluidity have been reported to accompany a number of disease processes.[58, 59] Remarkably, the administration of naringenin resulted in a substantial decrease of erythrocyte membrane fluidity in patients with essential hypertension, when compared to healthy controls.[12] Moreover, genistein and daidzein were also reported to reveal a softening effect on DOPC bilayers using a combination of X-ray scattering and MD simulations studies.[13] Our findings on the membrane-fluidizing effect in the presence of quercetin and rutin, correlates well with literature findings, which suggest the presence of flavonoids within the membrane leads to soften the membrane. Notwithstanding this view, some studies reported a rigidifying effect of membranes of fluid phase (L_α phase) with flavonoids.[60, 61] In Arora's study, the influence of several flavonoids, including rutin and naringenin on the fluidity of membranes composed of 1-stearoyl-2-linoleoyl-sn-glycero-3-phosphocholine (SLPC) was measured via anisotropic fluorescent microscopy. Apart from a membrane rigidifying effect, the authors suggested a localisation of the flavonoids in the hydrophobic core of the membranes.[60] Similarly, quercetin, rutin, naringenin and naringin at 20 mol% also induced rigidification of GUVs made of DOPC.[61]

The main reason why the findings in this context are quite diverse, is due to different flavonoid concentrations and membrane composition used. Reviewing literature suggests that when high concentrations of flavonoids are incorporated into more ordered bilayer with saturated hydrocarbon chains such as DPPC-based membranes, they create a fluidisation effect, whilst unsaturated lipid membranes such as DOPC-based systems mostly become more rigid. This biphasic effect of flavonoids on membrane lipids is similar to the influence observed with cholesterol.[53, 62] Cholesterol at 1-5 mol % induces a membrane fluidisation effect on POPC bilayers, whereas at higher cholesterol content, i.e., above 10 mol%, it rigidifies membranes.[63] These results imply that flavonoids may have some sort of "regulatory role" on membrane fluidity, in principle similar as cholesterol does. However we should keep in mind that flavonoids exist in the organism at much lower concentration than cholesterol, for which the biological role is more likely prevalent as membrane fluidizer.[9]

Molecular Areas of the Incorporated Flavonoids as Deduced from SAXS

The effective lateral area per molecule can then be determined using Eq. 4. The results of the lateral areas are summarized in **Figure 5**.

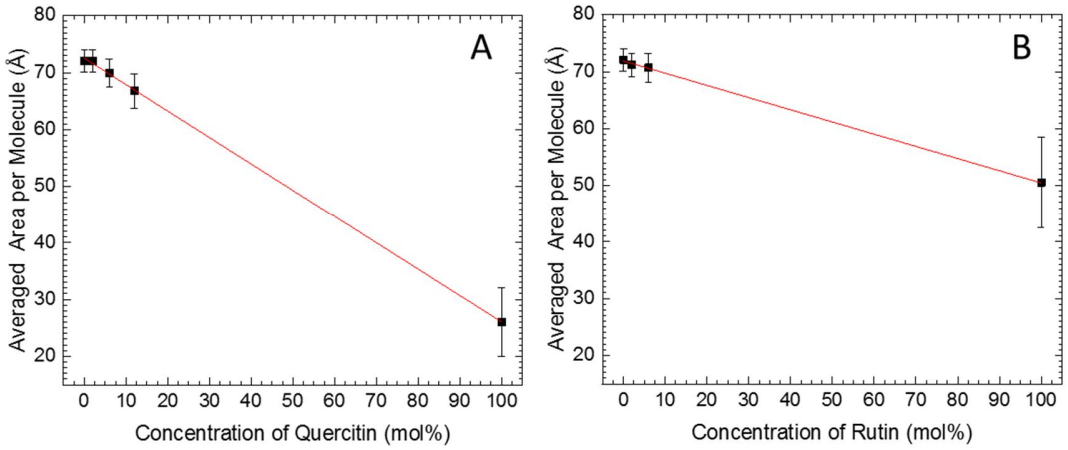

Figure 5. Effective lateral molecular area as a function of flavonoid concentration. Note, in the MD simulations of this study, this area is referred to as averaged area per molecule (APM).

Using the **Eq. 4**, we interpolated the effective lateral areas per molecule to 100% flavonoid concentration and obtained the partial molecular area of quercetin and rutin to be 26 ± 6 $Å^2$ and 51 ± 8 $Å^2$, respectively. Note, at 100% DOPC the area per lipid 72 ± 2 Å, which is in excellent agreement to the literature value of 72.5 $Å^2$ at 30 °C.[64] However, Langmuir-trough monolayer study by Ferreira *et al.* determined the area per quercetin molecule as A_{flav} = 89 $Å^2$ at π = 20 mN m^{-1}.[65] Although the two values seem to be contradicting to each other (26 *vs* 89 $Å^2$), this difference might arise from the different orientations of quercetin molecule at two different interfaces. At the air water interface, quercetin molecules might preferentially align in a way with the rings oriented mainly parallel to the water surface. A parallel oriented quercetin molecule would have the largest projected area. However, when incorporated into the membrane at full hydration, occupied in-plane surface area by quercetin is close to the smallest possible projected area.

Positioning of Flavonoids in DOPC Bilayers by MD Simulations

The two flavonoids inserted and partitioned in lipid bilayer at different locations, according to the presence (or not) of sugar moieties and charge state. Standalone quercetin located below the high lipid-density polar head region, at 12.2 ± 2.2 Å from the membrane centre (namely, lipid bilayer centre of mass, COM, see Table 3a and Figure S8 and S9 in the Supporting Information). This position is driven by H-bonding interaction between the OH-groups of quercetin and the polar head groups of DOPC. Concerning rutin, the sugar moiety pulled the flavonoid moiety towards water-membrane interface, and the COM of this moiety located at 15.6 ± 1.8 Å (see Table 3a). The rutin glucose and rhamnose moieties located at 17.8 ± 2.2 Å and 16.0 ± 2.0 Å from the membrane centre, respectively. Due to their polar and H-bond donor/acceptor features, sugar moieties tightly anchored rutin to the polar head region, maximising noncovalent interactions with phosphatidylcholines (see Figure 6 top).

As expected, and previously observed with other derivatives,[66, 67, 68] the phenolate forms of both derivatives exhibit superficial insertion in the bilayer, owing to strong noncovalent electrostatic interactions between the anionic polyphenol moiety and the choline moieties of the membrane ($\langle z_{Flavonoid} \rangle$ = 15.8 ± 1.8 Å and 16.1 ± 1.9 Å for quercetin and rutin, respectively, see **Table 3a**). Consequently, the sugar moieties of anionic flavonoids inserted slightly deeper than for their neutral counterparts. It is highly expected that the flavonoids approach membrane in their anionic form and re-protonate at membrane surface (see **Figure 6 bottom**). In this region, pK_a values are probably modified to facilitate neutral forms and subsequent insertion.

Table 3. Average distances of characteristic moieties with respect to the membrane centre of mass (COM) (in Å) in (a) 1.5 mol% and (b) 12 mol% enriched quercetin- and rutin-DOPC systems.

(a)	**Quercetin:DOPC**		**Rutin:DOPC**	
Moiety	**Neutral**	**Anionic**	**Neutral**	**Anionic**
Flavonoid	12.2 ± 2.2	15.8 ± 1.8	15.6 ± 1.8	16.1 ± 1.9
Glucose	-	-	17.8 ± 2.2	17.1 ± 1.9
Rhamnose	-	-	16.0 ± 2.0	13.0 ± 2.0

(b)	**Quercetin:DOPC**	**Rutin:DOPC**
Flavonoid	13.6 ± 2.1	13.7 ± 2.0
Glucose	-	16.4 ± 2.6
Rhamnose	-	16.3 ± 3.0

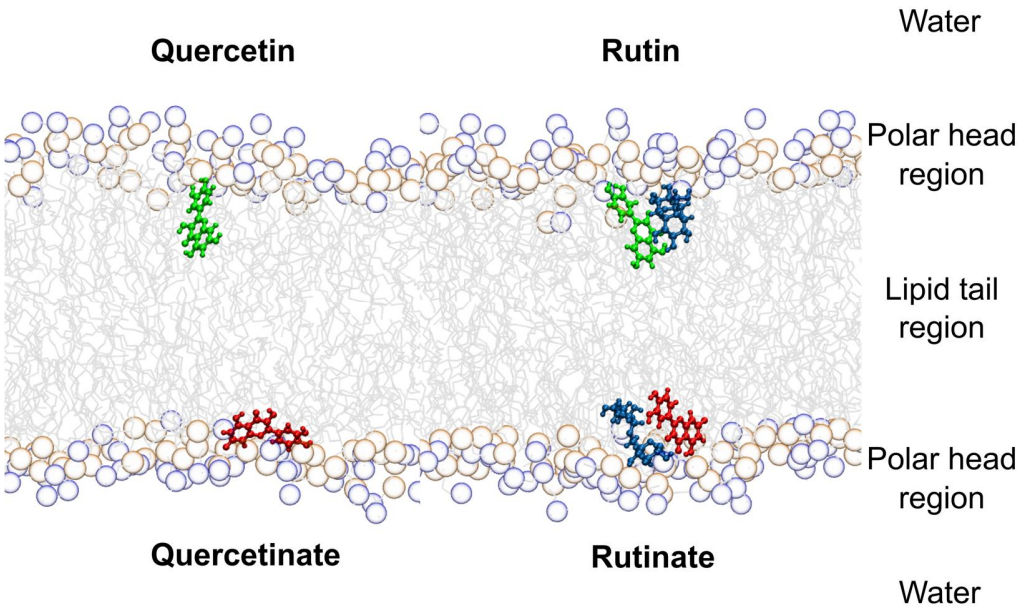

Figure 6. Representative snapshots of positioning of quercetin and rutin (1.5 mol%) in a DOPC membrane model. The flavonoid moieties are depicted in green and red for neutral and charged species, respectively; the sugar moieties are coloured in blue.

With high flavonoid concentrations (12 mol%), the depth of insertion was significantly affected with respect to the lower concentration (1.5 mol%) situation, as $\langle z_{Flavonoid} \rangle$ was 13.6 ±

2.1 Å and 13.7 ± 2.0 Å for quercetin and rutin, respectively (see Table 3b). The sugar moieties of rutin were still in close contact with the polar head region (see Table 3b and Figure 7). However, these differences observed with respect to the flavonoid concentration suggest a dramatic reorganisation of lipid bilayer structure in the presence of large number of flavonoid molecules (see below for further details). Only a few self-association events (i.e., noncovalent flavonoid dimers) were observed in the 12 mol% quercetin-DOPC systems along MD simulations. However, such events have been repeatedly described with polyphenols in water,[69] and were also seen between polyphenols and vitamin E in lipid bilayers.[63] Due to differences in solvophobic effects in both water and lipid environments, π-π stacking interaction between aromatic polyphenol moieties is more likely to happen in water. However, such interactions may also happen in lipid bilayer when increasing concentration, thus initiating the formation of polyphenol nanodomains. When increasing concentration, bigger aggregates are likely to be formed, in agreement with aforementioned SAXS experiments wherein crystallization was observed above 24 mol%.

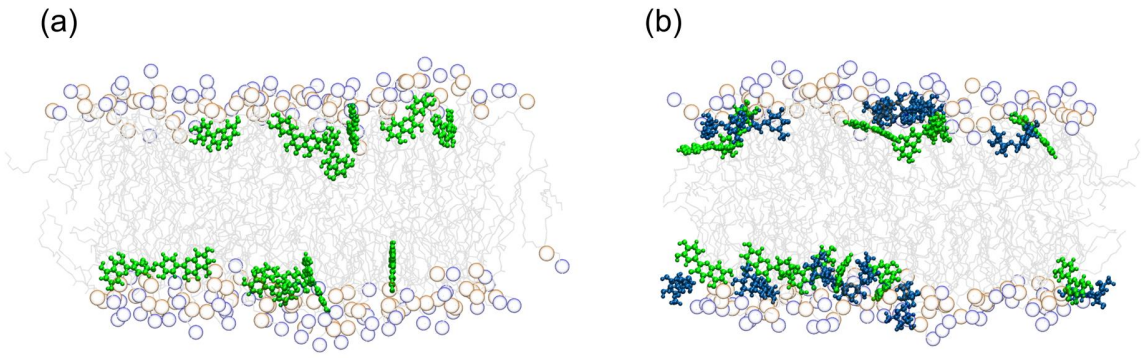

Figure 7. Representative snapshots of (a) quercetin-DOPC and (b) rutin-DOPC (12 mol%) from MD simulations. Polyphenol and sugar moieties are depicted in green, blue, respectively.

The current view for the localisation of quercetin and rutin within the biomimetic membranes correlates well with other existing studies, which suggest localisation of flavonoids between the phospholipid/water interface and the upper half of the hydrocarbon chain region.[28, 70, 71, 72, 73] Some studies instead report that the flavonoids partition into the hydrophobic region of the membrane, [60, 61] which is unexpected regarding the amphiphilic character of quercetin and rutin, and also because their OH groups are prone to form hydrogen bonds with the polar head groups. An extensive NMR study using POPC MLVs as model system supports this notion of flavonoid's localisation at the lipid/water interface with the OH groups tendency to hydrogen bond to the polar headgroup moieties.[72] As we observed here, Movileanu *et al.*[70] observe a pH-dependent insertion of quercetin within membranes. That is, quercetin molecules inserted between the polar head groups at alkaline pH and with a deeper location at acidic pH (cp. **Table 3A**). This is related to the pK_a of flavonoids, where the phenolate form cannot insert deep in the membrane and locates closer to polar interface (cp. **Figure 7**). Conversely, at acidic pH, the protonated (neutral) form is predominant, allowing the flavonoid to insert deeper in the membrane. Košinová and co-workers confirmed this trend by MD simulations, showing that for the protonated forms of quercetin and its metabolites, the 3-OH, 3'-OH, 4'-OH and keto groups were localised at 15 ± 2 Å from the membrane centre,[52] thus orienting the flavonoid moiety more parallel to the surface. Rutin-membrane interactions have also been studied via infrared (IR) spectroscopy. The frequency shift of OH and keto groups indicated rutin associated with the polar end of the phospholipids.[74]

Orientation of Flavonoids in DOPC Bilayers by MD Simulation

The orientation of the flavonoid moieties in lipid bilayer membrane were assessed in terms of the α-angle defined between the membrane normal *z*-axis and the B-ring-to-A-ring vector (see

Figure 1). Quercetin appears slightly tilted from the parallel to the membrane surface (α-angle ca. 60° with great flexibility, see Figure S2 in the Supporting Information). The α-angle profile of its (non-inserted) anionic form is broader (Figure S2), due to the numerous possibilities of interatomic (noncovalent) interactions providing greater flexibility at the membrane surface. Rutin behaves differently due to its sugar moiety, which anchors the molecule to the polar head group region and drives the flavonoid moiety more perpendicular to membrane surface (α-angle of 30° ± 15°).

The α-angle profile of quercetin was similar with both 1.5 and 12 mol% quercetin to DOPC ratio, suggesting a low concentration dependence (Figure S2 and S3 in the Supporting Information). Conversely, for both rutin, the α-angle profiles were dramatically broadened (Figure S2 and S3), possibly due to significant changes in the lipid bilayer structure and a more bulky environment, when increasing rutin concentration.

Interactions between lipid polar heads and polyphenols can also be monitored by polyphenol-induced PC tilts (θ_{PC}). This was assessed by calculating the deviation of the angle between normal z-axis and the PC P-atom to N-atom vector according to the presence of quercetin or rutin molecules (below 20 Å, see, Table S3 in the Supporting Information).[75] At lower flavonoid concentration (1.5 mol%), PC heads were suggested to be strongly tilted in presence of polyphenols (27.5 ± 5.2° and 11.7 ± 5.2° for quercetin and rutin, respectively) in agreement with previous observations.[75] This might be attributed to the strong H-bond interactions between polyphenol OH groups and phosphate moieties, which in turn orient PC head towards small molecules. In the case of rutin, the presence of sugar moieties allows H-bond interactions directly in the polar head region, which distort less PC polar heads as pictured by a lower rutin-induced tilt with respect to quercetin. It is worth mentioning that polyphenol-induced PC tilt

heads cannot be statistically discussed for larger concentration (12%) since almost all PC heads are within 20 Å of polyphenol molecules. This, anyhow, strengthen the aforementioned hypothesis of global significant change in the lipid bilayer structure at this concentration (Table S3 in the Supporting Information).

Simulations of Flavonoid-Induced Membrane Structure Modifications

Even tough models consisting of ca. 128 molecules are not sufficiently big to comprehensively picture macroscopic lipid bilayer structural modifications, the calculated features provide hints. In the presence of 1.5 and 12 mol% quercetin, the lipid bilayer thickness, d_{HH} (measured as phosphate-phosphate distance) did not change significantly. The same accounts for also for 1.5 and 12 mol% of rutin: within errors no clear trend is displayed. That is, the overall thinning effect of flavonoids as seen with X-ray experiments cannot be confirmed, however, the absolute thickness values compare well to the results from Figure 3 and 4 (Table 4).

Although the two 1.5 mol% systems exhibited similar area per molecule (APM) of ca. 68 Å (Table 4), the 12 mol% quercetin-DOPC system exhibited a greater decrease in APM than with the 12 mol% rutin-DOPC system (<APM> being 62.0 and 63.7 $Å^2$, respectively, see Table 4). Note, that this trend is confirmed by the X-ray-based estimations, where we find <APMs> of 66 and 69 Å for 12 mol% quercetin and rutin, respectively (cp. Figure 5), i.e., quercetin displays clearly a smaller <APM> than rutin, and both flavonoids decrease APM values with increasing concentration.

Table 4. Averaged area per molecule (<APM>, in Å^2), DOPC membrane thickness, d_{HH} (in Å) and V_{tails} (kcal·mol^{-1}·atoms^{-1}) based on distance between P-atom density peaks. In brackets X-ray data at 25 °C from Figure 3, 4 and 5 are reported.

		<APM> (Å^2)	**d_{HH} (Å)**	**V_{tails}**
Quercetin	1.5 mol%	67.4 ± 1.1 (71 ± 2)	37.9 ± 0.5 (35.6 ± 0.2)	-0.508 ± 0.005
	12 mol%	62.0 ± 1.0 (66 ± 3)	38.2 ± 0.6 (35.1 ± 0.2)	-0.500 ± 0.006
Rutin	1.5 mol%	68.0 ± 1.1 (72 ± 2)	37.7 ± 0.5 (36.1 ± 0.2)	-0.529 ± 0.006
	12 mol%	63.7 ± 1.2 (69 ± 3)	37.4 ± 0.6 (35.6[1] ± 0.2)	-0.665 ± 0.006

[1] This d_{HH} value is actually determined at 6 mol% rutin. Note, at 12% we had already observed that rutin was not fully dissolvable in the membrane.

Inter-lipid interactions and lipid packing were assessed by V_{tails}, the average of potential noncovalent interaction energies (i.e., electrostatic and van der Waals interactions) between each lipid tail (i.e., the sn1- and sn2-tail chains up to the three glycerol atoms).[76, 77] The 12 mol% DOPC/rutin systems exhibited more attractive V_{tails} suggesting a stronger packing of DOPC lipid bilayer in the presence of large flavonoid concentrations (Table S5 in the Supporting Information). This is mainly attributed to more attractive electrostatic interactions in the lipid polar head region, due to the presence of rutin. This is confirmed by greater lipid order value in the upper part of the lipid tails (Figure S4 in the Supporting Information). To confirm the key role of electrostatic interactions, flavonoid-DOPC energies of interaction were split into three contributions: flavonoid-lipid, flavonoid-polar head and flavonoid-lipid tail noncovalent interaction energies (Table S4 in the Supporting Information). Electrostatic interactions with polar head groups clearly appears as the major contribution. This contribution is stronger with rutin due to increased electrostatic interactions with the sugar moiety. This contribution decreases in the 12 mol% systems due to a lower lipid density and thus less lipids surrounding the solutes, e.g., the energy of interaction between quercetin and polar head groups is -0.18 to -0.02 kcal·mol^{-1}· solute^{-1} with 1.5 mol% and 12 mol%, respectively (Table S4 in the Supporting

Information). To a lesser extent, flavonoid-lipid interactions are also driven by H-bonding between the OH-groups and the phosphatidylcholine moieties. This H-bond network is stronger with rutin since sugar moieties are strong H-atom donors and acceptors. Interestingly, this H-bond network is not concentration-dependent, the number of H-bond per molecule being similar for 1.5 mol% and 12 mol% systems (Figure S5 in the Supporting Information).

Conclusions

This work combines small angle X-ray scattering and MD simulations to determine structural and dynamic properties of DOPC bilayers in the presence of two prototypical flavonoids, quercetin and rutin. In a previous study,[10] we provided an overview on flavonoid interactions with planar membranes, ranking the extent of interactions in the order of quercetin > kaempferol > naringenin > hesperetin > catechin for flavonoid aglycones and tiliroside > rutin > naringin for flavonoid glycosides. Since quercetin clearly displayed stronger membrane interactions than rutin, we expected to observe this also in the nanostructural properties of flavonoid-loaded fluid bilayers. Some differences are indeed prevailing, while other trends are more subtle. Partial molecular areas of quercetin and rutin as well as the averaged molecular area per molecule, clearly show that rutin occupies an almost twice as big area in the head group region. Likewise, full solubility of rutin in DOPC membranes is reached already at 6 mol%, which is only half of that of quercetin. Further, it is tempting to assume that both flavonoids induce an increase in membrane fluidity, since membrane undulations and membrane thinning enhance monotonously with the flavonoid's concentration. Again, quercetin showing a subtle, but significantly stronger effect than rutin. MD results display further differences: the flavonoid moieties of quercetin and

rutin are located at a depth of 12 and 16 Å, respectively, as rutin is more anchored to the polar head group surface by its sugar moiety. Their phenolate (anionic) forms display a location closer to the polar interface. Quercetin displays are more tilted orientation of 60° with respect to the bilayer normal, whereas rutin is oriented more perpendicular (α-angle 30°). Finally, at all concentrations studied rutin induces a stronger attractive electrostatic interaction between the polar lipid head groups due to its presence in this interfacial region.

Acknowledgments

Dr Sanver would like to thank to the Ministry of National Education, Turkey for a PhD Grant. Dr Di Meo and Prof Trouillas thank CALI (CAlcul en Limousin) and Xavier Montagutelli for computational resources as well as Nouvelle Aquitaine Region and INSERM for financial support.

References

1. Azevedo, M. I.; Pereira, A. F.; Nogueira, R. B.; Rolim, F. E.; Brito, G. A.; Wong, D. V. T.; Lima-Júnior, R. C.; de Albuquerque Ribeiro, R.; Vale, M. L. The antioxidant effects of the flavonoids rutin and quercetin inhibit oxaliplatin-induced chronic painful peripheral neuropathy. *Molecular pain* **2013,** *9*, 1744-8069-9-53.
2. Tang, S.-M.; Deng, X.-T.; Zhou, J.; Li, Q.-P.; Ge, X.-X.; Miao, L. Pharmacological basis and new insights of quercetin action in respect to its anti-cancer effects. *Biomedicine & Pharmacotherapy* **2020,** *121*, 109604.
3. Ren, N.; Kim, E.; Li, B.; Pan, H.; Tong, T.; Yang, C. S.; Tu, Y. Flavonoids alleviating insulin resistance through inhibition of inflammatory signaling. *J Agr Food Chem* **2019,** *67* (19), 5361-5373.
4. Kawabata, K.; Mukai, R.; Ishisaka, A. Quercetin and related polyphenols: new insights and implications for their bioactivity and bioavailability. *Food & function* **2015,** *6* (5), 1399-1417.
5. Kapešová, J.; Petrásková, L.; Markošová, K.; Rebroš, M.; Kotik, M.; Bojarová, P.; Křen, V. Bioproduction of quercetin and rutinose catalyzed by rutinosidase: novel concept of "solid state biocatalysis". *International journal of molecular sciences* **2019,** *20* (5), 1112.
6. Castell, M.; J Perez-Cano, F.; Abril-Gil, M.; Franch, A. Flavonoids on allergy. *Current pharmaceutical design* **2014,** *20* (6), 973-987.
7. Jucá, M. M.; Cysne Filho, F. M. S.; de Almeida, J. C.; Mesquita, D. d. S.; Barriga, J. R. d. M.; Dias, K. C. F.; Barbosa, T. M.; Vasconcelos, L. C.; Leal, L. K. A. M.; Ribeiro, J. E.; Vasconcelos, S. M. M. Flavonoids: biological activities and therapeutic potential. *Natural Product Research* **2020,** *34* (5), 692-705.
8. Huang, M.; Su, E.; Zheng, F.; Tan, C. Encapsulation of flavonoids in liposomal delivery systems: the case of quercetin, kaempferol and luteolin. *Food & function* **2017,** *8* (9), 3198-3208.
9. Sadeghpour, A.; Sanver, D.; Rappolt, M. Interactions of flavonoids with lipidic mesophases. In *Advances in Biomembranes and Lipid Self-Assembly*; Elsevier B.V., 2017; Vol. 25, pp 95-123.
10. Sanver, D.; Murray, B. S.; Sadeghpour, A.; Rappolt, M.; Nelson, A. L. Experimental Modeling of Flavonoid-Biomembrane Interactions. *Langmuir* **2016,** *32* (49), 13234-13243.
11. Rappolt, M. 50 Years of structural lipid bilayer modelling. In *Advances in Biomembranes and Lipid Self-Assembly*, Iglic, A.; Rappolt, M.; Garcia-Saez, A. J., Eds.; Elsevier B.V., 2019; Vol. 29, pp 1-21.
12. Ajdžanović, V.; Jakovljević, V.; Milenković, D.; Konić-Ristić, A.; Živanović, J.; Jarić, I.; Milošević, V. Positive effects of naringenin on near-surface membrane fluidity in human erythrocytes. *Acta Physiologica Hungarica* **2015,** *102* (2), 131-136.
13. Raghunathan, M.; Zubovski, Y.; Venable, R. M.; Pastor, R. W.; Nagle, J. F.; Tristram-Nagle, S. Structure and Elasticity of Lipid Membranes with Genistein and Daidzein Bioflavinoids Using X-ray Scattering and MD Simulations. *The Journal of Physical Chemistry B* **2012,** *116* (13), 3918-3927.
14. Hung, W.-C.; Chen, F.-Y.; Lee, C.-C.; Sun, Y.; Lee, M.-T.; Huang, H. W. Membrane-thinning effect of curcumin. *Biophys. J.* **2008,** *94* (11), 4331-4338.
15. Sanver, D.; Murray, B. S.; Sadeghpour, A.; Rappolt, M.; Nelson, A. L. Experimental Modeling of Flavonoid–Biomembrane Interactions. *Langmuir* **2016,** *32* (49), 13234-13243.

16. Huang, T. C.; Toraya, H.; Blanton, T. N.; Wu, Y. X-ray powder diffraction analysis of silver behenate, a possible low-angle diffraction standard. *J. Appl. Crystallogr.* **1993,** *26*, 180-184.
17. Pabst, G.; Rappolt, M.; Amenitsch, H.; Laggner, P. Structural information from multilamellar liposomes at full hydration: full q-range fitting with high quality x-ray data. *Physical review. E, Statistical physics, plasmas, fluids, and related interdisciplinary topics* **2000,** *62* (3 Pt B), 4000-9.
18. Rappolt, M.; Pabst, G. Flexibility and structure of fluid bilayer interfaces. Wiley Online Library, 2008, pp 45-81.
19. Kennedy, J.; Eberhart, R. In *Particle swarm optimization*, Proceedings of ICNN'95-International Conference on Neural Networks, 1995; IEEE, pp 1942-1948.
20. Pabst, G.; Rappolt, M.; Amenitsch, H.; Laggner, P. Structural information from multilamellar liposomes at full hydration: full q-range fitting with high quality x-ray data. *Physical Review E* **2000,** *62* (3), 4000-4009.
21. Pabst, G.; Katsaras, J.; Raghunathan, V. A.; Rappolt, M. Structure and Interactions in the Anomalous Swelling Regime of Phospholipid Bilayers. *Langmuir* **2003,** *19*, 1716-1722.
22. Rappolt, M.; Pabst, G. Flexibility and structure of fluid bilayer interfaces. In *Structure and dynamics of membranous interfaces*, Nag, K., Ed.; John Wiley & Sons: Hoboken, 2008, pp 45-81.
23. Rappolt, M. Bilayer thickness estimations with "poor" diffraction data. *J.Appl.Phys.* **2010,** *107*, 084701-1-084701-7.
24. Caillé, A. Remarques sur la diffusion des rayons X dans les smectiques A. *C.R.Acad.Sc.Paris B* **1972,** *274*, 891-893.
25. Zhang, R.; Suter, R. M.; Nagle, J. F. Theory of the structure factor of lipid bilayers. *Phys.Rev.E* **1994,** *50* (6), 5047-5060.
26. De Gennes, P. G.; Prost, J. *The physics of liquid crystals*; 2nd edition ed.; Oxford University Press: Oxford, 1993.
27. Petrache, H. I.; Tristram-Nagle, S.; Nagle, J. F. Fluid phase structure of EPC and DMPC bilayers. *Chemistry and physics of lipids* **1998,** *95* (1), 83-94.
28. Hodzic, A.; Zoumpoulakis, P.; Pabst, G.; Mavromoustakos, T.; Rappolt, M. Losartan's affinity to fluid bilayers modulates lipid–cholesterol interactions. *Phys Chem Chem Phys* **2012,** *14* (14), 4780-4788.
29. Pool, H.; Mendoza, S.; Xiao, H.; McClements, D. J. Encapsulation and release of hydrophobic bioactive components in nanoemulsion-based delivery systems: Impact of physical form on quercetin bioaccessibility. *Food and Function* **2013,** *4* (1), 162-174.
30. Nagle, J. F.; Tristram-Nagle, S. Structure and interactions of lipid bilayer: role of fluctuations. In *Lipid bilayers. Structure and interactions*, Katsaras, J.; Gutberlet, T., Eds.; Springer: Berlin, 2000, pp 1-23.
31. Nagle, J. F.; Tristram-Nagle, S. Structure of lipid bilayers. *Biochimica Et Biophysica Acta-Reviews on Biomembranes* **2000,** *1469* (3), 159-195.
32. Chiu, S. W.; Jakobsson, E.; Mashl, R. J.; Scott, H. L. Cholesterol-induced modifications in lipid bilayers: a simulation study. *Biophys.J.* **2002,** *83*, 1842-1853.
33. Tristram-Nagle, S.; Petrache, H. I.; Nagle, J. F. Structure and interactions of fully hydrated dioleoylphosphatidylcholine bilayers. *Biophys. J.* **1998,** *75* (2), 917-925.

34. Pan, J.; Tristram-Nagle, S.; Kučerka, N.; Nagle, J. F. Temperature dependence of structure, bending rigidity, and bilayer interactions of dioleoylphosphatidylcholine bilayers. *Biophys. J.* **2008,** *94* (1), 117-124.
35. Dickson, C. J.; Madej, B. D.; Skjevik, Å. A.; Betz, R. M.; Teigen, K.; Gould, I. R.; Walker, R. C. Lipid14: The Amber Lipid Force Field. *J. Chem. Theory Comput.* **2014,** *10* (2), 865-879.
36. Price, D. J.; Brooks, C. L. A modified TIP3P water potential for simulation with Ewald summation. *J. Chem. Phys.* **2004,** *121* (20), 10096-10103.
37. Wang, J.; Wolf, R. M.; Caldwell, J. W.; Kollman, P. A.; Case, D. A. Development and testing of a general amber force field. *J. Comput. Chem.* **2004,** *25* (9), 1157-1174.
38. Wang, J.; Wang, W.; Kollman, P. A.; Case, D. A. Automatic atom type and bond type perception in molecular mechanical calculations. *Journal of Molecular Graphics & Modelling* **2006,** *25*, 247-260.
39. Duan, Y.; Wu, C.; Chowdhury, S.; Lee, M. C.; Xiong, G.; Zhang, W.; Yang, R.; Cieplak, P.; Luo, R.; Lee, T.; Caldwell, J.; Wang, J.; Kollman, P. A point-charge force field for molecular mechanics simulations of proteins based on condensed-phase quantum mechanical calculations. *J. Comput. Chem.* **2003,** *24*, 1999-2012.
40. Frisch, M. J.; Trucks, G. W.; Schlegel, H. B.; Scuseria, G. E.; Robb, M. A.; Cheeseman, J. R.; Scalmani, G.; Barone, V.; Mennucci, B.; Petersson, G. A.; Nakatsuji, H.; Caricato, M.; Li, X.; Hratchian, H. P.; Izmaylov, A. F.; Bloino, J.; Zheng, G.; Sonnenberg, J. L.; Hada, M.; Ehara, M.; Toyota, K.; Fukuda, R.; Hasegawa, J.; Ishida, M.; Nakajima, T.; Honda, Y.; Kitao, O.; Nakai, H.; Vreven, T.; Montgomery, J. A.; Peralta, J. E.; Ogliaro, F.; Bearpark, M.; Heyd, J. J.; Brothers, E.; Kudin, K. N.; Staroverov, V. N.; Kobayashi, R.; Normand, J.; Raghavachari, K.; Rendell, A.; Burant, J. C.; Iyengar, S. S.; Tomasi, J.; Cossi, M.; Rega, N.; Millam, J. M.; Klene, M.; Knox, J. E.; Cross, J. B.; Bakken, V.; Adamo, C.; Jaramillo, J.; Gomperts, R.; Stratmann, R. E.; Yazyev, O.; Austin, A. J.; Cammi, R.; Pomelli, C.; Ochterski, J. W.; Martin, R. L.; Morokuma, K.; Zakrzewski, V. G.; Voth, G. A.; Salvador, P.; Dannenberg, J. J.; Dapprich, S.; Daniels, A. D.; Farkas; Foresman, J. B.; Ortiz, J. V.; Cioslowski, J.; Fox, D. J. Gaussian 09, Revision A.02. Wallingford CT, 2009.
41. Dupradeau, F.-Y.; Pigache, A.; Zaffran, T.; Savineau, C.; Lelong, R.; Grivel, N.; Lelong, D.; Rosanski, W.; Cieplak, P. The R.E.D. Tools: Advances in RESP and ESP charge derivation and force field library building. *Phys. Chem. Chem. Phys.* **2010,** *12*, 7821-7839.
42. Kirschner, K. N.; Yongye, A. B.; Tschampel, S. M.; González-Outeiriño, J.; Daniels, C. R.; Foley, B. L.; Woods, R. J. GLYCAM06: A generalizable biomolecular force field. Carbohydrates. *J. Comput. Chem.* **2008,** *29* (4), 622-655.
43. Jo, S.; Kim, T.; Iyer, V. G.; Im, W. CHARMM-GUI: A web-based graphical user interface for CHARMM. *J. Comput. Chem.* **2008,** *29*, 1859-1865.
44. Case, D. A.; Betz, R. M.; Botello-Smith, W.; Cerutti, D. S.; III, T. E. C.; Darden, T. A.; Duke, R. E.; Giese, T. J.; Gohlke, H.; Goetz, A. W.; Homeyer, N.; Izadi, S.; Janowski, P.; Kaus, J.; Kovalenko, A.; Lee, T. S.; LeGrand, S.; Li, P.; Lin, C.; Luchko, T.; Luo, R.; Madej, B.; Mermelstein, D.; Merz, K. M.; Monard, G.; Nguyen, H.; Nguyen, H. T.; Omelyan, I.; Onufriev, A.; Roe, D. R.; Roitberg, A.; Sagui, C.; Simmerling, C. L.; Swails, J.; Walker, R. C.; Wang, J.; Wolf, R. M.; Wu, X.; Xiao, L.; York, D. M.; Kollman, P. A. *AMBER16*, University of California, San Francisco., 2016.
45. Salomon-Ferrer, R.; Case, D. A.; Walker, R. C. An overview of the Amber biomolecular simulation package. *WIREs Comp. Mol. Sci.* **2013,** *3* (2), 198-210.

46. Nagle, J. F.; Petrache, H. I.; Gouliaev, N.; Tristram-Nagle, S.; Liu, Y.; Suter, R. M.; Gawrisch, K. Multiple mechanisms for critical behavior in the biologically relevant phase of lecithin bilayers. *Physical Review E* **1998,** *58* (6), 7769.
47. Vogel, M.; Münster, C.; Fenzl, W.; Salditt, T. Thermal unbinding of highly oriented phospholipid membranes. *Phys Rev Lett* **2000,** *84* (2), 390.
48. Pabst, G.; Katsaras, J.; Raghunathan, V. Enhancement of steric repulsion with temperature in oriented lipid multilayers. *Phys Rev Lett* **2002,** *88* (12), 128101.
49. Drasler, B.; Drobne, D.; Sadeghpour, A.; Rappolt, M. Fullerene up-take alters bilayer structure and elasticity: A small angle X-ray study. *Chemistry and Physics of Lipids* **2015,** *188* (0), 46-53.
50. Kobayashi, Y.; Fukada, K. Characterization of swollen lamellar phase of dimyristoylphosphatidylcholine–gramicidin A mixed membranes by DSC, SAXS, and densimetry. *Biochimica et Biophysica Acta (BBA)-Biomembranes* **1998,** *1371* (2), 363-370.
51. Pabst, G.; Amenitsch, H.; Kharakoz, D. P.; Laggner, P.; Rappolt, M. Structure and fluctuations of phosphatidylcholines in the vicinity of the main phase transition. *Phys.Rev.E* **2004,** *70*, 021908-1-021908-9.
52. Košinová, P. n.; Berka, K.; Wykes, M.; Otyepka, M.; Trouillas, P. Positioning of antioxidant quercetin and its metabolites in lipid bilayer membranes: implication for their lipid-peroxidation inhibition. *The Journal of Physical Chemistry B* **2012,** *116* (4), 1309-1318.
53. Saija, A.; Scalese, M.; Lanza, M.; Marzullo, D.; Bonina, F.; Castelli, F. Flavonoids as antioxidant agents: Importance of their interaction with biomembranes. *Free Radical Biology and Medicine* **1995,** *19* (4), 481-486.
54. Pawlikowska-Pawlęga, B.; Gruszecki, W. I.; Misiak, L.; Paduch, R.; Piersiak, T.; Zarzyka, B.; Pawelec, J.; Gawron, A. Modification of membranes by quercetin, a naturally occurring flavonoid, via its incorporation in the polar head group. *Biochimica et Biophysica Acta (BBA)-Biomembranes* **2007,** *1768* (9), 2195-2204.
55. Sun, Y.; Hung, W.-C.; Chen, F.-Y.; Lee, C.-C.; Huang, H. W. Interaction of tea catechin (—)-epigallocatechin gallate with lipid bilayers. *Biophys. J.* **2009,** *96* (3), 1026-1035.
56. How, C. W.; Teruel, J. A.; Ortiz, A.; Montenegro, M. F.; Rodríguez-López, J. N.; Aranda, F. J. Effects of a synthetic antitumoral catechin and its tyrosinase-processed product on the structural properties of phosphatidylcholine membranes. *Biochimica et Biophysica Acta (BBA)-Biomembranes* **2014,** *1838* (5), 1215-1224.
57. Elliott, J.; Needham, D.; Dilger, J.; Haydon, D. The effects of bilayer thickness and tension on gramicidin single-channel lifetime. *Biochimica et Biophysica Acta (BBA)-Biomembranes* **1983,** *735* (1), 95-103.
58. Harroun, T. A.; Heller, W. T.; Weiss, T. M.; Yang, L.; Huang, H. W. Experimental evidence for hydrophobic matching and membrane-mediated interactions in lipid bilayers containing gramicidin. *Biophys. J.* **1999,** *76* (2), 937-945.
59. Ingolfsson, H. I.; Koeppe, R. E.; Andersen, O. S. Curcumin is a modulator of bilayer material properties. *Biochemistry* **2007,** *46* (36), 10384-10391.
60. Arora, A.; Byrem, T. M.; Nair, M. G.; Strasburg, G. M. Modulation of Liposomal Membrane Fluidity by Flavonoids and Isoflavonoids. *Arch Biochem Biophys* **2000,** *373* (1), 102-109.
61. Tedeschi, A.; D'Errico, G.; Lauro, M. R.; Sansone, F.; Di Marino, S.; D'Ursi, A. M.; Aquino, R. P. Effect of flavonoids on the Aβ(25-35)-phospholipid bilayers interaction. *European Journal of Medicinal Chemistry* **2010,** *45* (9), 3998-4003.

62. Poklar Ulrih, N.; Ota, A.; Šentjurc, M.; Kure, S.; Abram, V. Flavonoids and cell membrane fluidity. *Food Chemistry* **2010,** *121* (1), 78-84.
63. Rappolt, M.; Vidal, M. F.; Kriechbaum, M.; Steinhart, M.; Amenitsch, H.; Bernstorff, S.; Laggner, P. Structural, dynamic and mechanical properties of POPC at low cholesterol concentration studied in pressure/temperature space. *European Biophysics Journal with Biophysics Letters* **2003,** *31* (8), 575-585.
64. Kucerka, N.; Tristram-Nagle, S.; Nagle, J. F. Structure of fully hydrated fluid phase lipid bilayers with monounsaturated chains. *J.Membrane Biol.* **2005,** *208*, 193-202.
65. Ferrreira, J. V. N.; Grecco, S. d. S.; Lago, J. H. G.; Caseli, L. Ultrathin films of lipids to investigate the action of a flavonoid with cell membrane models. *Materials Science and Engineering: C* **2015,** *48* (0), 112-117.
66. Fabre, G.; Bayach, I.; Berka, K.; Paloncýová, M.; Starok, M.; Rossi, C.; Duroux, J. L.; Otyepka, M.; Trouillas, P. Synergism of antioxidant action of vitamins E, C and quercetin is related to formation of molecular associations in biomembranes. *Chemical Communications* **2015,** *51* (36), 7713-7716.
67. Ossman, T.; Fabre, G.; Trouillas, P. Interaction of wine anthocyanin derivatives with lipid bilayer membranes. *Comput. Theor. Chem.* **2016,** *1077*, 80-86.
68. Valentová, K.; Káňová, K.; Di Meo, F.; Pelantová, H.; Chambers, C. S.; Rydlová, L.; Petrásková, L.; Křenková, A.; Cvačka, J.; Trouillas, P.; Křen, V. Chemoenzymatic preparation and biophysical properties of sulfated Quercetin metabolites. *International Journal of Molecular Sciences* **2017,** *18* (11).
69. Charlton, A. J.; Baxter, N. J.; Khan, M. L.; Moir, A. J. G.; Haslam, E.; Davies, A. P.; Williamson, M. P. Polyphenol/peptide binding and precipitation. *Journal of Agricultural and Food Chemistry* **2002,** *50* (6), 1593-1601.
70. Movileanu, L.; Neagoe, I.; Flonta, M. L. Interaction of the antioxidant flavonoid quercetin with planar lipid bilayers. *Int J Pharm* **2000,** *205* (1–2), 135-146.
71. Ollila, F.; Halling, K.; Vuorela, P.; Vuorela, H.; Slotte, J. P. Characterization of Flavonoid–Biomembrane Interactions. *Arch Biochem Biophys* **2002,** *399* (1), 103-108.
72. Scheidt, H. A.; Pampel, A.; Nissler, L.; Gebhardt, R.; Huster, D. Investigation of the membrane localization and distribution of flavonoids by high-resolution magic angle spinning NMR spectroscopy. *Biochimica et Biophysica Acta (BBA)-Biomembranes* **2004,** *1663* (1), 97-107.
73. Pawlikowska-Pawlęga, B.; Dziubińska, H.; Król, E.; Trębacz, K.; Jarosz-Wilkołazka, A.; Paduch, R.; Gawron, A.; Gruszecki, W. I. Characteristics of quercetin interactions with liposomal and vacuolar membranes. *Biochimica et Biophysica Acta (BBA) - Biomembranes* **2014,** *1838* (1, Part B), 254-265.
74. Singh, D.; SM Rawat, M.; Semalty, A.; Semalty, M. Rutin-phospholipid complex: an innovative technique in novel drug delivery system-NDDS. *Current drug delivery* **2012,** *9* (3), 305-314.
75. Kiriakidi, S.; Chatzigiannis, C.; Papaemmanouil, C.; Tzakos, A. G.; Mavromoustakos, T. Exploring the role of the membrane bilayer in the recognition of candesartan by its GPCR AT1 receptor. *Biochimica et Biophysica Acta (BBA) - Biomembranes* **2020,** *1862* (3), 183142.
76. Di Meo, F.; Fabre, G.; Berka, K.; Ossman, T.; Chantemargue, B.; Paloncýová, M.; Marquet, P.; Otyepka, M.; Trouillas, P. In silico pharmacology: Drug membrane partitioning and crossing. *Pharmacological Research* **2016,** *111*, 471-486.

77. Wennberg, C. L.; Van Der Spoel, D.; Hub, J. S. Large influence of cholesterol on solute partitioning into lipid membranes. *J. Am. Chem. Soc.* **2012,** *134* (11), 5351-5361.

Table of Content